Photodegradation of Chlorophenoxyacetic Acids by ZnO/γ-Fe$_2$O$_3$ Nanocatalysts: A Comparative Study

Abdul Halim Abdullah[1,2], Lee Kian Mun[1], Zulkarnain Zainal[1] & Mohd Zobir Hussein[2]

[1] Deparment of Chemistry, Faculty of Science, Universiti Putra Malaysia, Serdang, Selangor, Malaysia

[2] Institute of Advanced Technology, Universiti Putra Malaysia, Serdang, Selangor, Malaysia

Correspondence: Abdul Halim Abdullah, Deparment of Chemistry, Faculty of Science, Universiti Putra Malaysia, 43400 Serdang, Selangor, Malaysia. Tel: 1-603-8946-6603. E-mail: halim@upm.edu.my

Abstract

ZnO/γ-Fe$_2$O$_3$ nanocomposite was synthesized via simple precipitation. The synthesized nanocatalysts underwent heat treatment at 450 $^{\circ}$C for an hour. The characteristics of the nanocomposite were investigated by XRD, TEM, and BET surface area measurement. Zeta potential analysis was used to examine the surface charge properties of the nanocatalysts. The synthesized nanocomposite has an average particle size of 11 nm and a surface area of 20 m^2 g^{-1}. The potential of ZnO/γ-Fe$_2$O$_3$ as a photocatalyst was evaluated by photodegrading chlorophenoxyacetic acids (PAA, 2,4-D, 2,4,5-T and 4CA). The decomposition of chlorophenoxyacetic acids by ZnO/γ-Fe$_2$O$_3$ followed 4CA > 2,4,5-T ≈ 2,4-D > PAA. The result indicates the applicability of ZnO/γ-Fe$_2$O$_3$ nanocomposite as a photocatalyst in removing organic pollutants in wastewater.

Keywords: photocatalytic degradation, precipitation, zinc oxide, 2,4-D

1. Introduction

Rapid industrialisation has resulted in, among other things, problems with water pollution. The discharge of wastewater and chemical spillage into water channels has exacerbated the water quality crisis (Richardson, 2008; Wintgens, Salehi, Hochstrat, & Melin, 2008). Although many conventional methods have been applied in removing organic contaminants, those methods do not lead to total mineralisation of the pollutants. Moreover, further treatment is needed since the methods employed are unable to convert the pollutants into harmless products such as CO$_2$ and H$_2$O, which indirectly increases the operational cost (Allegre, Maisseu, Charbit, & Moulin, 2004; Gaya & Abdullah, 2008; Lu, Zhang, Ma, & Chen, 2009; Padmanabhan et al., 2006; Yang & Cheng, 2007). Therefore, the development of an efficient wastewater treatment solution is imperative.

Semiconductor photocatalysis has received increased attention due to its inherent ability to lead to complete mineralisation of organic carbon into carbon dioxide and water (Erquez & Pichat, 2006; Kaneco, Itoh, Katsumata, Suzuki, & Ohta, 2009; Kaniou, Pitarakis, Barlagianni, & Poulios, 2009; Pera-Titus, García-Molina, Baños, Giménez, & Esplugas, 2004; Rao, Sivasankar, & Sadasivam, 2005; Uddin, Hasnat, Samed, & Majumdar, 2007) without a mass transfer. Moreover, this process can be performed under ambient conditions using atmospheric oxygen as the oxidant (Chatterjee & Dasgupta, 2005).

One of the major drawbacks in semiconductor photocatalysis is the recombination of photogenerated holes (h$^+$) and electrons (e$^-$). This recombination step lowers the quantum yield and wastes energy. Therefore, the e$^-$-h$^+$ recombination process should be inhibited to ensure efficient photocatalysis. Coupled semiconductors have been proven to enhance the charge separation of electron-hole pairs, which increases the lifetime of the charge carriers and consequently reduces the recombination of electron-hole pairs (Serpone, Maruthamuthu, Pichat, Pelizzetti, & Hidaka, 1995). This is based on the fact that the photogenerated electrons can flow from one semiconductor with a higher to a lower conduction band minimum. Under such conditions, the separation of electron-hole pairs was promoted while keeping reduction and oxidation reactions at two different sites (Peng, Xie, Lu, Fan, & Wang, 2010; Shang et al., 2009; Wang et al., 2009). As a result, the efficiency of semiconductors improved (Jing, Xu, Sun, Jing, & Cai, 2001; Lin, Wu, Zhang, & Pan, 2009; Liu, Ye, Xiong, & Liu, 2010; Vaezi, 2008; Zheng et al., 2009).

The widespread use of chlorophenoxyacetic acids as herbicides in agriculture has raised public concern due to

the accumulation of disposed residues in natural waters (Bucheli, Grüebler, Müller, & Schwarzenbach, 1997). There have been many studies on the removal of chlorophenoxy herbicides using titanium dioxide (Bahnemann, Muneer, & Haque, 2007; Giri, Ozaki, Ishida, Takanami, & Taniguchi, 2007; Kamble, Sawant, & Pangarkar, 2006; Singh, Saquib, Haque, & Muneer, 2007; Tanaka & Reddy, 2002) Very little work involved ZnO (Djebbar & Sehili, 1998). Since ZnO has almost the same band gap energy (3.2 eV) as TiO_2, its photocatalytic capability is anticipated to be similar to that of TiO_2. Moreover, ZnO is relatively cheaper compared to TiO_2 whereby the usage of TiO_2 and platinum catalyst are uneconomic for large scale water treatment operations (Daneshvar, Salari, & Khataee, 2004). The greatest advantage of ZnO over TiO_2 is the ability to absorb a wide range of solar spectrum (Behnajady, Modirshahla, & Hamzavi, 2006). Based on these factors, we synthesized $ZnO/\gamma\text{-}Fe_2O_3$ and evaluated its potential as photocatalyst. To our best knowledge, no works have been carried out by $ZnO/\gamma\text{-}Fe_2O_3$ on the removal of the selected chlorophenoxyacetic acids. In this paper, $ZnO/\gamma\text{-}Fe_2O_3$ nanocomposites were obtained via precipitation. The characteristics of the resulting catalysts and their efficiency in degrading chlorophenoxyacetic acids were studied. The ease of degradation of chlorophenoxy herbicides by $ZnO/\gamma\text{-}Fe_2O_3$ was also studied.

2. Method

2.1 Reagents and Apparatus

Zinc acetate dihydrate ($Zn(CH_3COO)_2 \cdot 2H_2O$), ammonia solution (25% v/v, $NH_3 \cdot H_2O$) and 4-chlorophenoxyacetic acid ($C_8H_7ClO_3$) were obtained from Merck. Iron acetate ($Fe(CH_3COO)_2$) and phenoxyacetic acid ($C_8H_8O_3$) were purchased from Aldrich. 2,4-dichlorophenoxyacetic acid ($C_8H_6Cl_2O_3$) and 2,4,5-trichlorophenoxyacetic acid ($C_8H_5Cl_3O_3$) were obtained from Fluka. All the chemicals were used without any purification. Deionized water was used throughout the study.

2.2 Synthesis and Characterization of ZnO/γ-Fe₂O₃ Nanocomposite

0.01 mole of $Zn(CH_3COO)_2 \cdot 2H_2O$ and 0.001 mole of $Fe(CH_3COO)_2$ were dissolved in 100 mL deionized water at room temperature. Ammonia solution was added drop-wise into the zinc-iron solution with vigorous stirring to ensure homogenous formation of precipitate. The precipitate was centrifuged, washed with deionized water and oven-dried overnight at 110 ^{o}C. The resulting powder was then calcined at 450 ^{o}C for an hour in a box furnace (Carbolite, CWF 1200).

The obtained products were characterized by XRD (Shimazdu XRD-6000 Diffractometer), TEM (Hitachi 7100) and BET surface area (Autosorb AS-1, Quantachrome). ImageJ, a free software package was used to measure the particle size of the catalyst based on TEM micrographs while SPSS software (IBM) was applied in constructing the particle size distribution histogram. The band gap of the synthesized catalysts was determined by UV-Vis diffuse reflectance spectrometry. The surface charge of $ZnO/\gamma\text{-}Fe_2O_3$ was measured by a zeta potential analyzer (Zetasizer Nano series, Malvern Instruments).

2.3 Photodegradation Experiments

The photodegradation efficiency of the synthesized $ZnO/\gamma\text{-}Fe_2O_3$ nanocomposite was evaluated by photodegrading chlorophenoxyacetic acids in a photoreactor under 6 W UV-A irradiation (365 nm, Hitachi). In a typical experiment, appropriate amounts of photocatalyst were suspended into 1 L solution of phenoxyacetic acid in a photoreactor. Where required, the pH of the solution was adjusted by the addition of HNO_3 or NaOH. The solution was stirred for 15 min at 280 rpm to attain adsorption equilibrium prior to irradiation. During irradiation, agitation was maintained by a magnetic stirrer and air was bubbled into the reaction medium to ensure a constant supply of oxygen (2 L min^{-1}). Other factors such as temperature and light intensity were held constant. 5 mL samples were withdrawn at regular time intervals for 4 hours and were immediately filtered by 0.45 μm cellulose nitrate filters to remove catalyst particles. The concentration of chlorophenoxyacetic acids in test samples was determined by a Perkin Elmer Lambda 35 UV-Vis spectrophotometer.

3. Results

3.1 Characterization of ZnO/γ-Fe₂O₃ Nanocomposite

Figure 1 depicts the XRD patterns of the synthesized $ZnO/\gamma\text{-}Fe_2O_3$ nanocomposite. It can be seen that the XRD patterns of the $ZnO/\gamma\text{-}Fe_2O_3$ exhibit the typical pattern of hexagonal ZnO (JCPDS card no.: 36-1451) and cubic $\gamma\text{-}Fe_2O_3$ (JCPDS card no.: 39-1346). No other impurity peaks were detected.
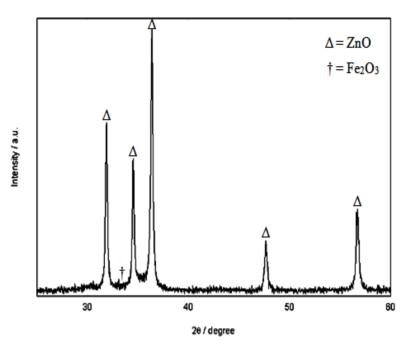
Figure 1. XRD patterns of ZnO/γ-Fe$_2$O$_3$ nanocomposite

Figure 2(a) is the TEM micrograph of ZnO/γ-Fe$_2$O$_3$. The nanoparticles were spherical with an average size of 11 nm, as determined from the particle size distribution histogram (Figure 2(b)). The surface area of the ZnO/γ-Fe$_2$O$_3$ nanocomposite was 20 m^2 g^{-1}. This agrees with TEM analysis, where small particle sizes result in a large surface area. The synthesized ZnO/γ-Fe$_2$O$_3$ catalyst has band gap energy of 3.11 eV (Figure 3). In order to study the surface properties of the ZnO/γ-Fe$_2$O$_3$ nanocomposite, the electrokinetics of the composite were measured as zeta potentials as a function of pH. The pH of point of zero charge (pH$_{zpc}$) of the nanocatalyst was 7.3, indicating that the catalyst surface is positively charged below pH 7.3 and is negatively charged when the pH value is greater than 7.3 (Figure 4).
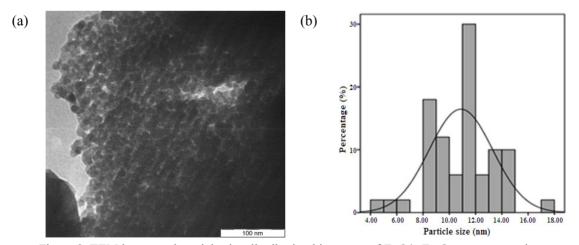
(a)

(b)

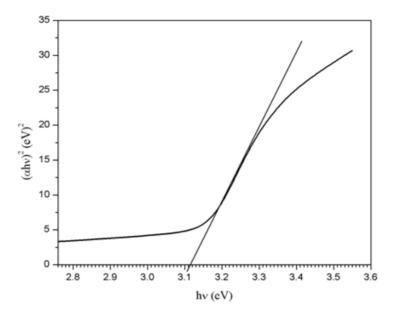Figure 2. TEM image and particle size distribution histogram of ZnO/γ-Fe$_2$O$_3$ nanocomposite

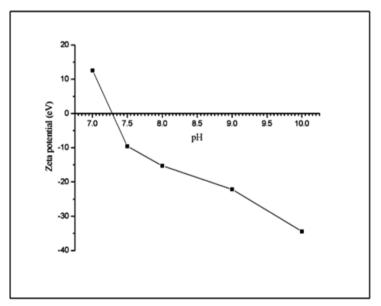Figure 3. Band gap energy plot of ZnO/γ-Fe$_2$O$_3$

Figure 4. Zeta potential curve of ZnO/γ-Fe$_2$O$_3$ as a function of pH

3.2 Photodegradation Studies

3.2.1 Preliminary Experiments

In order to validate the significant role of photocatalysis (UV/ZnO/γ-Fe$_2$O$_3$/ chlorophenoxyacetic acids) in the removal process, photolysis (UV/chlorophenoxyacetic acids) and adsorption (ZnO/γ-Fe$_2$O$_3$/ chlorophenoxyacetic acids) was performed as background experiments. The removal percentage of chlorophenoxyacetic acids was summarized in Table 1. It can be seen that there is no noticeable change in the concentration of chlorophenoxyacetic acids either in photolysis or adsorption test except for photocatalysis. Thus, there is a synergistic effect between the ZnO/γ-Fe$_2$O$_3$ catalyst and UV irradiation for the photodegradation process to work effectively.

Table 1. Removal of chlorophenoxyacetic acids under various experimental conditions

Pollutant	Percentage of removal (%)		
	Photolysis	Adsorption	Photocatalysis
2,4-D	0.97	1.98	55.29
2,4,5-T	0.48	2.90	57.00
PAA	1.40	3.24	47.17
4CA	2.86	2.73	59.43

Experimental conditions: Photocatalyst loading = 0.20 g L^{-1}, pollutant concentration = 20 mg L^{-1}.

3.2.2 Effect of Photocatalyst Loading

The effect of ZnO/γ-Fe$_2$O$_3$ dosage on the removal of chlorophenoxyacetic acids was examined at an initial concentration of 20 mg L^{-1}. A series of experiments were performed while varying only the amount of photocatalyst from 0.20 to 0.60 g (Figure 5). The percentage of photodegradation initially increased with the amount of catalyst loaded and then decreased beyond optimum mass. This phenomenon is based on the fact that the increase in catalyst dosage also increases the total active surface area and the number of reaction sites (L.Wei, Shifu, Z. Wei, & Sujuan, 2009). As a result, the number of hydroxyl and superoxide radicals increases as well, which facilitates the degradation of the pollutant. Thus, the degradation percentage is enhanced. However, a reduction in photodegradation was observed when the photocatalyst dosage went beyond the optimum concentration (0.4 g L^{-1} for 2,4-D and 2,4,5-T and 0.5 g L^{-1} for PAA and 4CA). This may be due to the opacity of the solution, reducing UV light penetration, which consequently reduces degradation of the pollutant (Pardeshi & Patil, 2008). Furthermore, the low percentage of degradation may due to the agglomeration of ZnO/γ-Fe$_2$O$_3$ which causes a reduction in catalyst surface area available for light and pollutant adsorption and suppresses the generation of hydroxyl radicals (Daneshvar et al., 2004).
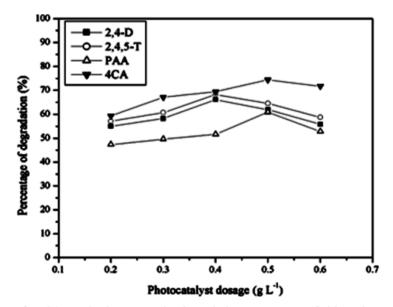

Figure 5. Effect of ZnO/γ-Fe$_2$O$_3$ dosage on the degradation percentage of chlorophenoxyacetic acids

3.2.3 Effect of Substrate Concentration

The influence of pollutant concentration on the degradation rate of the chlorophenoxyacetic acids was studied in the range of 10 to 50 mg L^{-1} at their respective optimum catalyst dosages. The rate of reaction is given by:

$$r_1 = -dC/dt = k_1C \tag{1}$$

where r_1, C and k_1 are the rate of reaction, the concentration of chlorophenoxyacetic acids and the first-order rate constant, respectively. Integration of Equation 1 gives:

$$ln(C_0/C)=k_1t \tag{2}$$

where C_o is the initial concentration of the chlorophenoxyacetic acids and t is irradiation time.

The first-order rate constant (k_1) is determined from the slope of the linear plots of ln (C_0/C) versus irradiation time, t. The first-order rate constant, k_1 and correlation factor, R^2 values are shown in Table 2. The high value of R^2 indicates the degradation of chlorophenoxyacetic acids follow first-order kinetics. The rate of reaction increased with increasing chlorophenoxyacetic acid concentration up to the optimum concentration and then decreased at higher concentrations (Figure 6). This may be due to the screening effect of the pollutant molecules, which reduced light penetration of the solution. Moreover, the generated intermediates may also compete with the pollutant molecules for the hydroxyl radicals. Thus, the photodegradation efficiency reduced as the substrate concentration increased (Khataee & Zarei, 2011). Additionally, the active sites are also covered by adsorbed pollutant molecules and intermediates that can reduce hydroxyl radical generation (Konstantinou & Albanis, 2004). Therefore, the concentration of hydroxyl radicals is insufficient to photodegrade the pollutants at higher concentrations. Another possibility is that the catalyst dosage, light intensity and irradiation period are constant as the initial concentrations of pollutants increases. Thus, the number of hydroxyl radicals formed on the catalyst surface is also constant. Hence, the hydroxyl radicals available to degrade substrate molecules would decrease at higher pollutant concentrations leading to a decrease in degradation. Another possible factor that could lead to the above phenomena is the competition between adsorbed pollutant molecules and water molecules for the photogenerated holes (Gaya & Abdullah, 2008).

Table 2. First-order rate constant, k_1 and R^2 values of various initial chlorophenoxyacetic acids concentrations

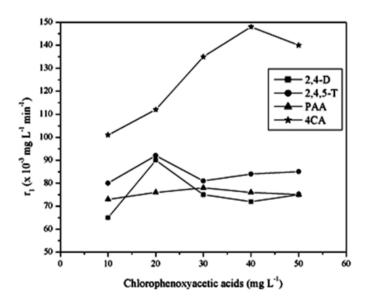| Concentration	2,4-D		2,4,5-T		PAA		4CA	
(mg L^{-1})	k_1	R^2	k_1	R^2	k_1	R^2	k_1	R^2
10	6.5	0.9896	8.0	0.9684	7.3	0.9960	10.1	0.9959
20	4.5	0.9861	4.6	0.9881	3.8	0.9907	5.6	0.9968
30	2.5	0.9831	2.7	0.9811	2.6	0.9942	4.5	0.9837
40	1.8	0.9834	2.1	0.9983	1.9	0.9962	3.7	0.9966
50	1.5	0.9866	1.7	0.9940	1.5	0.9922	2.8	0.9860

Figure 6. First-order rate of chlorophenoxyacetic acids at different concentrations

3.2.4 Effect of Initial pH

The influence of initial pH levels on the degradation performance of chlorophenoxyacetic acids was investigated at pH 5 to 10 (Figure 7). The results indicated that the photodecomposition rates of the chlorophenoxyacetic acids were low at pH 5 due to a substantial loss of ZnO.   A maximum degradation rate was observed at pH 7 and further increases in pH resulted in a lower removal efficiency. The pK_a of 2,4-D, 2,4,5-T, PAA and 4CA is 2.64, 2.88, 3.12 and 3.56, respectively. Therefore, the chlorophenoxyacetic acids are negatively charged above their respective pK_a values. As expected, the pH that shows optimal degradation must fall in between $pK_a < pH < pH_{zpc}$, due to the enhanced electrostatic interaction among the anions of the chlorophenoxyacetic acids and the positively charged catalyst surface (Daneshvar, Aber, Seyed-Dorraji, & Khataee, 2007). Above pH 7, the repulsive force between the negatively charged catalyst surface and the hydroxyl ions reduces the formation of hydroxyl radicals and consequently decreases the degradation rate (Qamar, Muneer, & Bahnemann, 2006). Is it notable that the hydroxyl radicals might act as a scavenging agent at high pH levels, which inhibits its reaction with the pollutant substrate (Davis & Huang, 1989). Hence, low removal percentage was observed at pH 10.
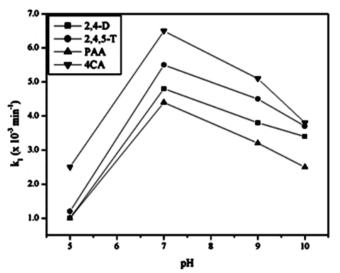

Figure 7. Effect of initial solution pH on the degradation rate of chlorophenoxyacetic acids

3.2.5 Degradation of Chlorophenoxyacetic Acids: A Comparison Study

Figure 8 shows the chemical structures of PAA, 2,4-D, 2,4,5-T and 4CA. Among the parameters studied, the percentage of photodegradation is in the following order: 4CA > 2,4,5-T ≈ 2,4-D > PAA. All chlorinated phenoxyacetic acids were degraded more than PAA. The corresponding byproducts of the reaction detected by UPLC were 4-chlorophenol, 2,4,5-trichlorophenol, 2,4-dichlorophenol and phenol, respectively. This indicates that the degradation process is driven by hydroxyl radicals. The attack of •OH on the CO position at the aromatic ring of PAA is not favorable, due to the stability of the benzene ring hence resulting in a low percentage of degradation. The present of chlorine, an ortho- and para- directing deactivators, will cause the •OH to attack the CO position of benzene ring, which is at the para position of the molecule in the case of 4CA. Conversely, 4CA was found to be the most degraded molecule among the studied chlorinated phenoxyacetic acids. Therefore the hydroxylation is the first elementary step which precedes the dissociation of chlorine atoms which is in agreement with Tang and Huang (1996). The increase in the number of chlorine atoms in the aromatic ring resulted in decreased degradation due to the steric effect. Additionally, the symmetrical and non existence of steric effect of 4CA may also contribute to the higher percentage of degradation (Kluson et al., 2008).
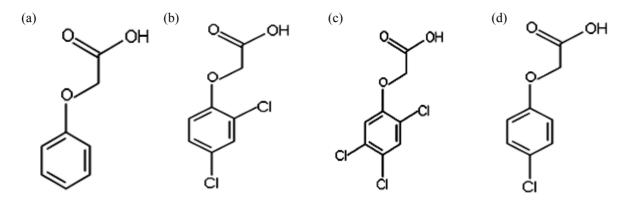
(a)   (b)   (c)   (d)

Figure 8. Chemical structure of (a) PAA, (b) 2,4-D, (c) 2,4,5-T and (d) 4CA

4. Conclusion

The highly photoactive $ZnO/\gamma\text{-}Fe_2O_3$ catalyst was successfully synthesized via precipitation followed by calcination at 450 °C for an hour. The photocatalyst produced was nearly spherical, has a surface area of 20 m^2 g^{-1}, an average particle size of 11 nm and a point of zero charge at pH 7.3. The efficiency of the synthesized $ZnO/\gamma\text{-}Fe_2O_3$ as a photocatalyst in photodegrading chlorophenoxy herbicides from aqueous solutions under UV irradiation increased with increasing mass of $ZnO/\gamma\text{-}Fe_2O_3$ up to an optimum loading but decreased at higher initial concentrations of the herbicides. The highest degradation percentage of chlorophenoxyacetic acids was achieved at pH 7. The ease of degradation of chlorophenoxyacetic acids was in the following order: 4CA > 2,4,5-T ≈ 2,4-D > PAA. Therefore, $ZnO/\gamma\text{-}Fe_2O_3$ nanocomposites have potential use in removing organic-polluted wastewater.

References

Allegre, C., Maisseu, M., Charbit, F., & Moulin, P. (2004). Coagulation–flocculation–decantation of dye house effluents: concentrated effluents. *Journal of Hazardous Materials, 116*(1-2), 57-64. http://dx.doi.org/10.1016/j.jhazmat.2004.07.005

Bahnemann, W., Muneer, M., & Haque, M. M. (2007). Titanium dioxide-mediated photocatalysed degradation of few selected organic pollutants in aqueous suspensions. *Catalysis Today, 124*(3-4), 133-148. http://dx.doi.org/10.1016/j.cattod.2007.03.031

Behnajady, M. A., Modirshahla, N., & Hamzavi, R. (2006). Kinetic study on photocatalytic degradation of C.I. Acid Yellow 23 by ZnO photocatalyst. *Journal of Hazardous Materials*, 133(1-3), 226-232. http://dx.doi.org/10.1016/j.jhazmat.2005.10.022

Bucheli, T. D., Grüebler, F. C., Müller, S. R., & Schwarzenbach, R. P. (1997). Simultaneous determination of neutral and acidic pesticides in natural waters at the low nanogram per liter level. *Analytical Chemistry*, 69(8), 1569-1576. http://dx.doi.org/10.1021/ac961059k

Chatterjee, D., & Dasgupta, S. (2005). Visible light induced photocatalytic degradation of organic pollutants. *Journal of Photochemistry and Photobiology C: Photochemistry Reviews, 6*(2-3), 186-205. http://dx.doi.org/10.1016/j.jphotochemrev.2005.09.001

Daneshvar, N., Aber, S., Seyed-Dorraji, M. S., Khataee, A. R., & Rasoulifard, M. H. (2007). Photocatalytic degradation of the insecticide diazinon in the presence of prepared nanocrystalline ZnO powders under irradiation of UV-C light. *Separation and Purification Technology, 58*(1), 91-98. http://dx.doi.org/10.1016/j.seppur.2007.07.016

Daneshvar, N., Salari, D., & Khataee, A. R. (2004). Photocatalytic degradation of azo dye Acid Red 14 in water on ZnO as an alternative catalyst to TiO₂. *Journal of Photochemistry and Photobiology A: Chemistry, 162*(2-3), 317-322. http://dx.doi.org/10.1016/S1010-6030(03)00378-2

Davis, A., & Huang, C. (1989). Removal of phenols from water by a photocatalytic oxidation process. *Water*

Science and Technology, 21(6-7), 455-464.

Djebbar, K., & Sehili, T. (1998). Kinetics of heterogeneous photocatalytic decomposition of 2,4-dichlorophenoxyacetic acid over titanium dioxide and zinc oxide in aqueous solution. *Pesticide Science, 54*(3), 269-276. http://dx.doi.org/10.1002/(SICI)1096-9063(1998110)54:3<269::AID-PS811>3.0.CO;2-I

Erquez, R., & Pichat, P. (2006). Different net effect of TiO_2 sintering temperature on the photocatalytic removal rates of 4-chlorophenol, 4-chlorobenzoic acid and dichloroacetic acid in water. *Journal of Environmental Science and Health Part A, 41*(6), 955-966. http://dx.doi.org/10.1080/10934520600689233

Gaya, U. I., & Abdullah, A. H. (2008). Heterogeneous photocatalytic degradation of organic contaminants over titanium dioxide: A review of fundamentals, progress and problems. *Journal of Photochemistry and Photobiology C: Photochemistry Reviews, 9*(1), 1-12. http://dx.doi.org/10.1016/j.jphotochemrev.2007.12.003

Giri, R. R., Ozaki, H., Ishida, T., Takanami, R., & Taniguchi, S. (2007). Synergy of ozonation and photocatalysis to mineralize low concentration 2,4-dichlorophenoxyacetic acid in aqueous solution. *Chemosphere, 66*(9), 1610-1617. http://dx.doi.org/10.1016/j.chemosphere.2006.08.007

Jing, L., Xu, Z., Sun, X., Jing, S., & Cai, W. (2001). The surface properties and photocatalytic activities of ZnO ultrafine particles. *Applied Surface Science, 180*(3-4), 308-314. http://dx.doi.org/10.1016/S0169-4332(01)00365-8

Kamble, S. P., Sawant, S. B., & Pangarkar, V. G. (2006). Photocatalytic mineralization of phenoxyacetic acid using concentrated solar radiation and titanium dioxide in slurry photoreactor. *Chemical Engineering Research and Design, 84*(5), 355-362. http://dx.doi.org/10.1205/cherd05011

Kaneco, S., Itoh, K., Katsumata, H., Suzuki, T., & Ohta, K. (2009). Titanium dioxide mediated solar photocatalytic degradation of thiram in aqueous solution: kinetics and mineralization. *Chemical Engineering Journal, 148*(1), 50-56. http://dx.doi.org/10.1016/j.cej.2008.07.029

Kaniou, S., Pitarakis, K., Barlagianni, I., & Poulios, I. (2005). Photocatalytic oxidation of sulfamethazine. *Chemosphere, 60*(3), 372-380. http://dx.doi.org/10.1016/j.chemosphere.2004.11.069

Khataee, A. R., & Zarei, M. (2011). Photocatalysis of a dye solution using immobilized ZnO nanoparticles combined with photoelectrochemical process. *Desalination, 273*(2-3), 453-460. http://dx.doi.org/10.1016/j.desal.2011.01.066

Kluson, P., Drobek, M., Krejcikova, S., Krysa, J., Kalaji, A., Cajthaml, T., & Rakusan, J. (2008). Molecular structure effects in photodegradation of phenol and its chlorinated derivatives with phthalocyanines. *Applied Catalysis B: Environmental, 80*(3-4), 321-326. http://dx.doi.org/10.1016/j.apcatb.2007.11.025

Konstantinou, I. K., & Albanis, T. A. (2004). TiO_2-assisted photocatalytic degradation of azo dyes in aqueous solution: kinetic and mechanistic investigations: A review. *Applied Catalysis B: Enviromental, 49*(1), 1-14. http://dx.doi.org/10.1016/j.apcatb.2003.11.010

Lin, D., Wu, H., Zhang, R., & Pan, W. (2009). Enhanced photocatalysis of electrospun Ag-ZnO heterostructured nanofibers. Chem. Mater*., 21*(15), 3479-3484. http://dx.doi.org/10.1021/cm900225p

Liu, R., Ye, H., Xiong, X., & Liu, H. (2010). Fabrication of TiO_2/ZnO composite nanofibers by electrospinning and their photocatalytic property. *Mater. Chem. Phys., 121*(3), 432-439. http://dx.doi.org/10.1016/j.matchemphys.2010.02.002

Lu, J., Zhang, T., Ma, J., & Chen, Z. (2009). Evaluation of disinfection by-products formation during chlorination and chloramination of dissolved natural organic matter fractions isolated from a filtered river water. *Journal of Hazardous Materials, 162*(1), 140-145. http://dx.doi.org/10.1016/j.jhazmat.2008.05.058

Padmanabhan, P. A. D., Sreekumar, K. P., Triyagarajan, T. K., Satpute, R. U., Bhanumurthy, K., Sengupta, P., . . . Warrier, K. G. K. (2006). Nano-crystalline titanium dioxide formed by reactive plasma synthesis. *Vacuum, 80*(11-12), 1252-1255. http://dx.doi.org/10.1016/j.vacuum.2006.01.054

Pardeshi, S. K., & Patil, A. B. (2008). A simple route for photocatalytic degradation of phenol in aqueous zinc oxide suspension using solar energy. *Solar Energy, 82*(8), 700-705. http://dx.doi.org/10.1016/j.solener.2008.02.007

Peng, L. L., Xie, T. F., Lu, Y. C., Fan, H. M., & Wang, D. J. (2010). Synthesis, photoelectric properties and photocatalytic activity of the Fe_2O_3/TiO_2 heterogeneous photocatalysts. *Physical Chemistry Chemical Physics, 12*, 8033-8041. http://dx.doi.org/10.1039/c002460k

Pera-Titus, M., García-Molina, V., Baños, M. A., Giménez, J., & Esplugas, S. (2004). Degradation of chlorophenols by means of advanced oxidation processes: a general review. *Applied Catalysis B: Environmental, 47*(4), 219-256. http://dx.doi.org/10.1016/j.apcatb.2003.09.010

Qamar, M., Muneer, M., & Bahnemann, D. (2006). Heterogeneous photocatalysed degradation of two selected pesticide derivatives, triclopyr and daminozid in aqueous suspensions of titanium dioxide. *Journal of Environment Management, 80*(2), 99-106. http://dx.doi.org/10.1016/j.jenvman.2005.09.002

Rao, A. N., Sivasankar, B., & Sadasivam, V. (2009). Kinetic study on the photocatalytic degradation of salicylic acid using ZnO catalyst. *Journal of Hazardous Materials, 166*(2-3), 1357-1361. http://dx.doi.org/10.1016/j.jhazmat.2008.12.051

Richardson, S. D. (2008). Environmental mass spectrometry: Emerging contaminants and current issues. *Analytical Chemistry, 80*(12), 4373-4402. http://dx.doi.org/10.1021/ac800660d

Serpone, N., Maruthamuthu, P., Pichat, P., Pelizzetti, E., & Hidaka, H. (1995). Exploiting the interparticle electron transfer process in the photocatalysed oxidation of phenol, 2-chlorophenol and pentachlorophenol: Chemical evidence for electron and hole transfer between coupled semiconductors. *Journal of Photochemistry and Photobiology A: Chemistry, 85*(3), 247-255. http://dx.doi.org/10.1016/1010-6030(94)03906-B

Shang, M., Wang, W. Z., Zhang, L., Sun, S. M., Wang, L., & Zhou, L. (2009). 3D Bi_2WO_6/TiO_2 hierarchical heterostructure: Controllable synthesis and enhanced visible photocatalytic degradation performances. *Journal of Physical Chemistry C, 113*(33), 14727-14731. http://dx.doi.org/10.1021/jp9045808

Singh, H. K., Saquib, M., Haque, M. M., & Muneer, M. (2007). Heterogeneous photocatalysed degradation of 4-chlorophenoxyacetic acid in aqueous suspensions. *Journal of Hazardous Materials, 142*(1-2), 374-380. http://dx.doi.org/10.1016/j.jhazmat.2006.08.032

Tanaka, K., & Reddy, K. S. N. (2002). Photodegradation of phenoxyacetic acid and carbamate pesticides on TiO_2. *Applied Catalysis B: Environmental, 39*(4), 305-310. http://dx.doi.org/10.1016/S0926-3373(02)00151-0

Tang, W. Z., & Huang, C. P. (1996). 2,4-oxidation kinetics by Fenton's reagent. *Environmental Technology, 17*(12), 1371-1378.

Uddin, M. M., Hasnat, M. A., Samed, A. J. F., & Majumdar, R. K. (2007). Influence of TiO_2 and ZnO photocatalysts on adsorption and degradation behaviour of erythrosine. *Dyes and Pigments, 75*(1), 207-212. http://dx.doi.org/10.1016/j.dyepig.2006.04.023

Vaezi, M. R. (2008). Two-step solochemical synthesis of ZnO/TiO_2 nano-composite materials. *J. Mater. Proc. Technol., 205*(1-3), 332-337. http://dx.doi.org/10.1016/j.jmatprotec.2007.11.122

Wang, X. W., Liu, G., Chen, Z. G., Li, F., Wang, L. Z., Lu, G. Q., & Cheng, H. M. (2009). Enhanced photocatalytic hydrogen evolution by prolonging the lifetime of carriers in ZnO/CdS heterostructures. *Chemical Communications*, 3452-3454. http://dx.doi.org/10.1039/b904668b

Wei, L., Shifu, C., Wei, Z., & Sujuan, Z. (2009). Titanium dioxide mediated photocatalytic degradation of methamidophos in aqueous phase. *Journal of Hazardous Materials, 164*(1), 154-160. http://dx.doi.org/10.1016/j.jhazmat.2008.07.140

Wintgens, T., Salehi, F., Hochstrat, R., & Melin, T. (2008). Emerging contaminants and treatment options in water recycling for indirect potable use. *Water Science and Technology, 57*(1), 99-107. http://dx.doi.org/10.2166/wst.2008.799

Yang, H., & Cheng, H. (2007). Controlling nitrite level in drinking water by chlorination and chloramination. *Separation and. Purification Technology, 56*(3), 392-396. http://dx.doi.org/10.1016/j.seppur.2007.05.036

Zheng, L. R., Zheng, Y. H., Chen, C. Q., Zhan, Y. Y., Lin, X. Y., Zheng, Q., . . . Zhu, J. F. (2009). Network structured SnO_2/ZnO heterojunction nanocatalyst with high photocatalytic activity. *Inorganic Chemistry, 48*(5), 1819-1825. http://dx.doi.org/10.1021/ic802293p

Copyrights